

Evidence of two kinds of acceptors in undoped semi-insulating GaAs: Positron trapping at gallium vacancies and negative ions

C. Le Berre and C. Corbel

Institut National des Sciences et Techniques Nucleaires, CE-Saclay, 91191 Gif-Sur-Yvette Cédex, France

K. Saarinen, S. Kuisma, and P. Hautojärvi

Laboratory of Physics, Helsinki University of Technology, 02150 Espoo, Finland

R. Fornari

Istituto Materiali Speciali per Elettronica e Magnetismo, Parma, Italy

(Received 6 March 1995)

Positron-lifetime experiments have been performed in Zn-doped *p*-type and undoped semi-insulating GaAs in the temperature range 20–300 K to investigate native point defects. In *p*-type materials with hole concentrations of 10^{15} – 10^{19} cm⁻³, no evidence of positron trapping is observed. The temperature dependence of the positron lifetime can be explained in terms of lattice expansion associated with positron-phonon coupling. Therefore, we ascribe it to delocalized positrons. In semi-insulating GaAs, two kinds of acceptors are detected with concentrations in the range 10^{15} – 10^{17} cm⁻³: gallium vacancies and negative ions. The temperature dependence of the positron trapping at the Ga vacancy exhibits a slope break at about 130 K. A weakly bound Rydberg-like precursor state is invoked to explain this temperature dependence.

I. INTRODUCTION

Native point defects introduce ionization levels in the back gap of semiconductors and interact with free carriers. Therefore, they have a strong influence on the electrical and optical properties of the materials. In undoped semi-insulating (SI) GaAs, the As-antisite-related EL2 defect, which as midgap donor can compensate the acceptors and pins the Fermi level at midgap, has been extensively studied, due to its technological importance.¹ However, the role of the other elementary defects such as vacancies is not clearly known because their identification is difficult. Very few experimental methods can provide direct information on the microscopic structure of the defects.

Because of its sensitivity to open volumes, charge states, and concentrations of the defects, positron annihilation is a powerful method to study vacancy-type defects in semiconductors.² Positrons are repelled by positive ion cores and positive vacancies, but they can localize at negative or neutral vacancy-type defects. The electron density at vacancies is reduced compared to the bulk. Therefore, the lifetime of trapped positrons is longer than that of positrons delocalized in the lattice. In *n*-type gallium arsenide, positron-lifetime spectroscopy has revealed As vacancies in the neutral or negative charge state, depending on the carrier concentration.³ The vacancies' concentration was estimated to be about 10^{16} – 10^{17} cm⁻³. In addition, negative ions were shown to trap positrons at Rydberg states at low temperatures. *p*-type materials were also studied, and no sign of positron trapping at vacancies was observed.³ The lifetime which was measured was the lowest for GaAs, 232 ps at 300 K, and very close to the theoretical value for delocalized positrons, 229 ps.⁴

It was thus attributed to positrons delocalized in the lattice. Much less study concerned semi-insulating substrates.

To investigate the role of vacancies in semi-insulating gallium arsenide, we have performed positron-lifetime experiments in various undoped SI GaAs substrates. As the positron-trapping rate calculation relies on the precise determination of the positron lifetime in the lattice and at defects, we have also performed measurements in heavily *p*-type doped materials to determine the positron lifetime in the lattice, $\tau_b(T)$, more accurately and at lower temperature than previously.³

We show in this paper that the temperature dependence in heavily *p*-type gallium arsenide can be explained in terms of thermal expansion and positron-phonon coupling. Such a dependence is characteristic of positrons delocalized in the lattice. We give evidence that positrons are trapped at negative vacancies, identified as V_{Ga} vacancies, and at negative ions in SI GaAs substrates. The positron-trapping coefficient at negative vacancies has a temperature dependence which can be explained by the two-stage positron capture model, via a Rydberg-like precursor state.⁵ We detect gallium vacancies in the range 10^{15} – 10^{16} cm⁻³. These concentrations are close to those of acceptors and EL2 defects, indicating that they indeed play a role in the compensation mechanism of undoped SI GaAs.

II. CRYSTALS, EXPERIMENTAL DETAILS, AND DATA ANALYSIS

A heavily *p*-type Zn-doped crystal was chosen with a carrier concentration equal to 10^{19} cm⁻³ at 300 K. This

TABLE I. The SI GaAs samples studied in this work, their neutral and total EL2 concentrations as calculated from infrared-absorption measurements, and their positron lifetimes at 20 K and room temperature.

Crystal	Supplier	Total [EL2] (cm ⁻³)	[EL2 ⁰] (cm ⁻³)	EL2 ⁺ fraction	$\bar{\tau}$ at 300 K (ps)	$\bar{\tau}$ at 20 K (ps)	τ_2 at 300 K (ps)
SI-GaAs No. 1	MASPEC	3.00×10^{16}	2.6×10^{16}	13%	234.9 ± 0.8	240.2 ± 0.8	260 ± 10
SI-GaAs No. 2	MASPEC	2.30×10^{16}	2.0×10^{16}	13%	235.4 ± 0.8	242.8 ± 0.8	258 ± 5
SI-GaAs No. 4	J. Matthey	1.04×10^{16}	9.7×10^{15}	7%	235.4 ± 0.8	239.6 ± 0.8	255 ± 6
SI-GaAs No. 3	MASPEC	1.10×10^{16}	1.0×10^{16}	9%	236.5 ± 0.8	243.6 ± 0.8	265 ± 4
SI-GaAs No. 7	MCP	not meas.	1.0×10^{16}		237.0 ± 0.8	237.5 ± 0.8	254 ± 5
SI-GaAs No. 6	J. Matthey	1.20×10^{16}	9.2×10^{15}	23%	237.4 ± 0.8	238.6 ± 0.8	260 ± 5
SI-GaAs No. 5	J. Matthey	1.04×10^{16}	9.1×10^{15}	12%	237.5 ± 0.8	241.4 ± 0.8	253 ± 5
SI-GaAs No. 8	Paderborn	2.20×10^{16}	1.8×10^{16}	18%	240.7 ± 0.8	240.1 ± 0.8	259 ± 4

concentration is very high, so that the Fermi level lies very close to the valence band. In that case, most of the ionization levels are depopulated and, thus, fewer defects are expected to trap positrons.

Eight pairs of samples (Nos. 1-8) of dimensions $5 \times 5 \times 0.4$ mm³, were cut from undoped SI GaAs wafers obtained from different suppliers (Johnson Matthey, Maspec, etc) and grown by the liquid-encapsulated Chro-zalski (LEC) method. Pair No. 8 was grown by the horizontal Bridgman (HB) method. Their total and neutral EL2 concentrations were measured using Fourier transform infrared (FTIR) absorption. They vary from 7×10^{15} to 3×10^{16} cm⁻³ with EL2⁺ fractions varying from 7% to 23%. All these data are tabulated in Table I.

The positron-lifetime spectra were recorded in darkness as a function of measurement temperature from 20 to 300 K, by using a fast-fast coincidence spectrometer with a full width at half maximum (FWHM) of 220 ps.² About 2.10^6 counts were collected for each spectrum. After source and background corrections, the lifetime spectra were analyzed with one or two exponential components. The average lifetime, calculated as $\bar{\tau} = \sum I_i \tau_i^*$ from the decomposed lifetimes τ_i^* and their intensities I_i , coincides with the center of the mass of the lifetime spectrum and is determined with a high accuracy of ± 0.8 ps.

From the data $\bar{\tau}$, τ_i^* and I_i , we determine the lifetimes associated with the different annihilation states using the conventional trapping model:² the bulk lifetime τ_b associated with delocalized positrons, and the lifetimes τ_{di} associated with the defects di which trap positrons. The average lifetime can be expressed as

$$\bar{\tau} = f_b \tau_b + \sum_i f_{di} \tau_{di}, \quad (1)$$

where f_j are the annihilation fractions in the different annihilation states. The trapping rate K_{di} at a defect di is proportional to the concentration C_{di} of the defect: $K_{di} = \mu_{di} C_{di}$, where μ_{di} is the positron trapping coefficient at the defect. The trapping rates K_{di} can be determined using the trapping model, as well as the annihilation fractions f_j , from the average lifetime $\bar{\tau}$, from the lifetimes in bulk τ_b , and at defects τ_{di} . The detection of lifetimes longer than τ_b is the fingerprint of vacancy-type defects.

III. POSITRON LIFETIME IN *p*-TYPE GaAs

A. Experimental results

In *p*-type GaAs, the lifetime spectra that were registered are one component, at all temperatures from 15 to 300 K. As seen in Fig. 1, the positron lifetime shows a plateau at low temperatures with a positron lifetime equal to 231.8 ± 0.8 ps. Above 175 K, the positron lifetime increases as a function of temperature and reaches the value 232.7 ± 0.8 ps at 300 K. A linear fit to the experimental lifetime in this region 175–300 K gives the result $\tau = 229.7$ ps + $(0.012$ ps/K) $[T(K) - 175]$. In Fig. 2, this behavior is compared to the data obtained in the previous work on three more lightly doped crystals, with carrier concentrations ranging from 5.4×10^{16} to 2×10^{18} cm⁻³. The four points measured below 175 K for these crystals are scattered around the plateau value. Those measured above 175 K can be fitted by the same linear expression that we obtain for the crystal *p*-type GaAs (10^{19} cm⁻³). We conclude that the temperature dependence of the pos-

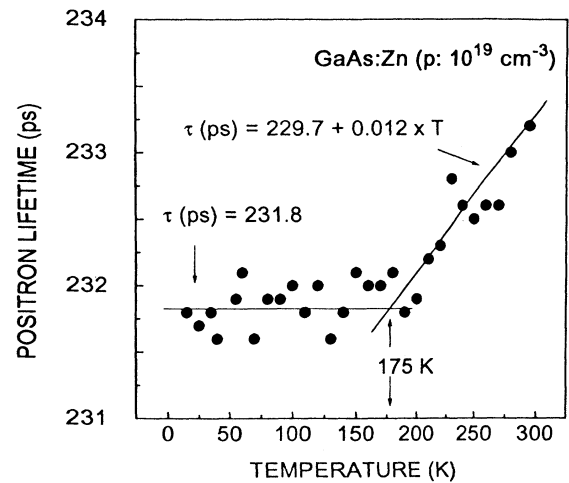


FIG. 1. Positron lifetime as a function of temperature in *p*-type Zn-doped GaAs with a carrier concentration $p = 10^{19}$ cm⁻³. Solid lines are linear fits of the experimental lifetime.

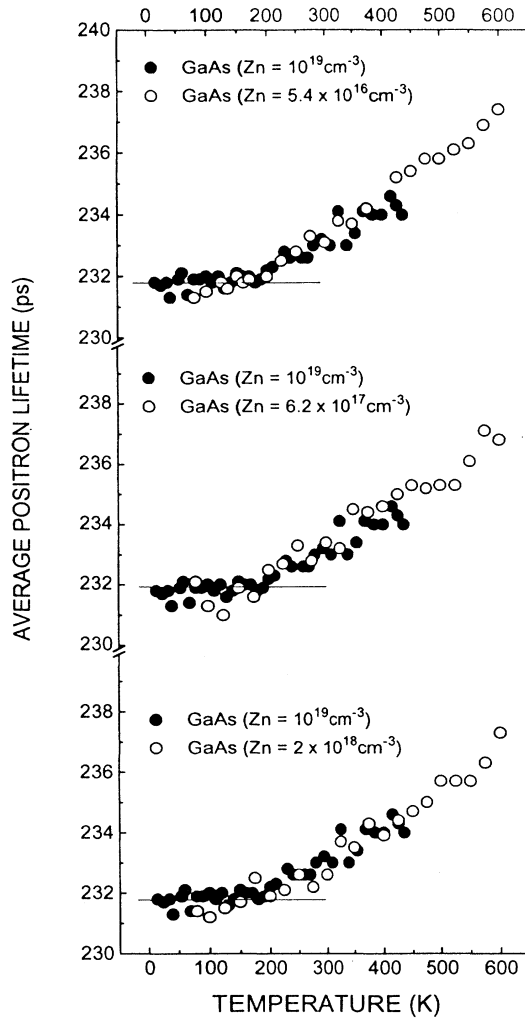


FIG. 2. Comparison between the positron lifetime measured in the crystal *p*-type GaAs (Zn: 10^{19} cm^{-3}) and measurements made in three less-doped crystals (Ref. 3).

itron lifetime is the same in the four *p*-type crystals with carrier concentrations ranging from 5.4×10^{16} to 10^{19} cm^{-3} .

B. Annihilation of positrons delocalized in the lattice

Positrons annihilate in *p*-type GaAs with lifetimes which from 20 to 600 K, independently of hole concentrations ranging from 5.4×10^{16} to $2 \times 10^{18} \text{ cm}^{-3}$, and are the lowest we measure in *p*-type materials. For such a range of temperature and hole (and consequently Zn) concentrations, if there is positron trapping one expects the fraction of trapped positrons to change. It follows that the lifetime of positrons, if they are trapped, is the same as in the delocalized state. There is consequently no evidence of positron trapping at vacancy-type defects. We can also conclude that if trapping at Zn acceptors takes place, it gives rise to the same lifetime as in the delocalized state. The temperature dependence is in-

dependent of hole (and consequently Zn) concentrations in *p*-type GaAs, and so reflects an intrinsic property of GaAs. To study if the temperature dependence of the positron lifetime in *p*-type GaAs can be ascribed to delocalized positrons, we have compared it to that of the lattice expansion. When the temperature increases sufficiently, the lattice expands and the electron density decreases. The positron-annihilation rate $\lambda = 1/\tau$ is proportional to the electron density, and thus inversely proportional to the crystal volume.² A theoretical value for the delocalized positron lifetime can then be written as²

$$\tau_{\text{th}} = \frac{a^3}{\sigma v N_a}, \quad (2)$$

where a^3 is the volume of the cubic cell, N_a is the number of electrons in this volume, σ is the cross section of the e^+e^- annihilation, and v is the e^+ velocity relatively to the electron. The changes of the cell parameter a are obtained from the thermal-expansion coefficient values given in Ref. 6. Figure 3 shows that the two parameters $\Delta\tau_{\text{exp}}/\tau_{\text{exp}}$ and $\Delta a^3/a^3$ present the same plateau at low temperatures, and that both increases as a function of temperature above 200 K. However, the experimental lifetime parameter increases more strongly. This difference can be explained if we take into account the positron-phonon coupling. According to Stott,⁷ lattice vibrations play a role in the positron distribution by temporarily expanding the interstitial spaces. The duration of these momentary expansions is long enough for positrons to annihilate, so that the electron density seen by positrons is lower than that due only to the continuous thermal expansion of the lattice.

We conclude that the temperature dependence of the positron lifetime can be explained in terms of thermal dilatation and positron-phonon coupling, and therefore is characteristic of that of positrons delocalized in the lat-

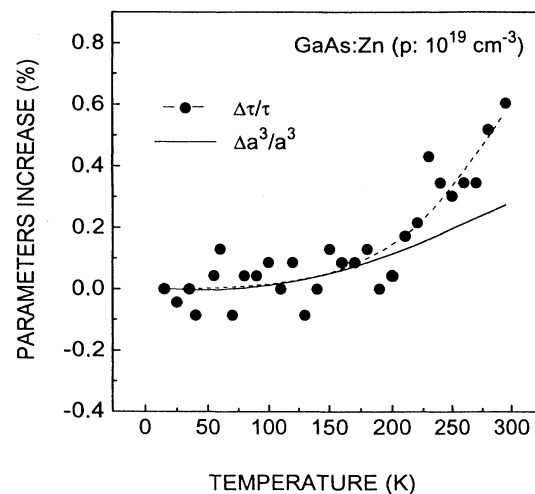


FIG. 3. Comparison between the thermal expansion of the lattice (cubic cell parameter a) and the increase of the positron lifetime τ in *p*-type GaAs (Zn: 10^{19} cm^{-3}). The dashed line is a guide for the eyes.

tice. In the following, a lifetime $\tau_b = 231.8$ ps will be used for trapping rate calculations at temperatures lower than 175 K. For temperatures greater or equal to 175 K, the expression of the linear fit in Fig. 1 will be used to determine τ_b .

IV. POSITRON LIFETIME IN SI GaAs

A. Experimental results

The average positron lifetime $\bar{\tau}$ in the SI GaAs crystals varies from 237 to 246 ps at 20 K and from 235 to 241 ps at 300 K (see Table I). For five of the eight crystals, Nos. 1–5, the average lifetime $\bar{\tau}$ decreases continuously from 20 to 300 K, as shown in Fig. 4. For the three others, Nos. 6–8, $\bar{\tau}$ goes through a minimum in the temperature range 50–100 K and then tends to level off between 100 and 300 K. Regarding the lifetime spectra decompositions shown in Fig. 5, the crystals can be divided in two groups. In the first group of four crystals, including Nos. 1–4, the longest exponential component τ_2 is constant from 20 to 300 K with the value 258 ± 5 ps. In the second group of four crystals, including Nos. 5–8, the decompo-

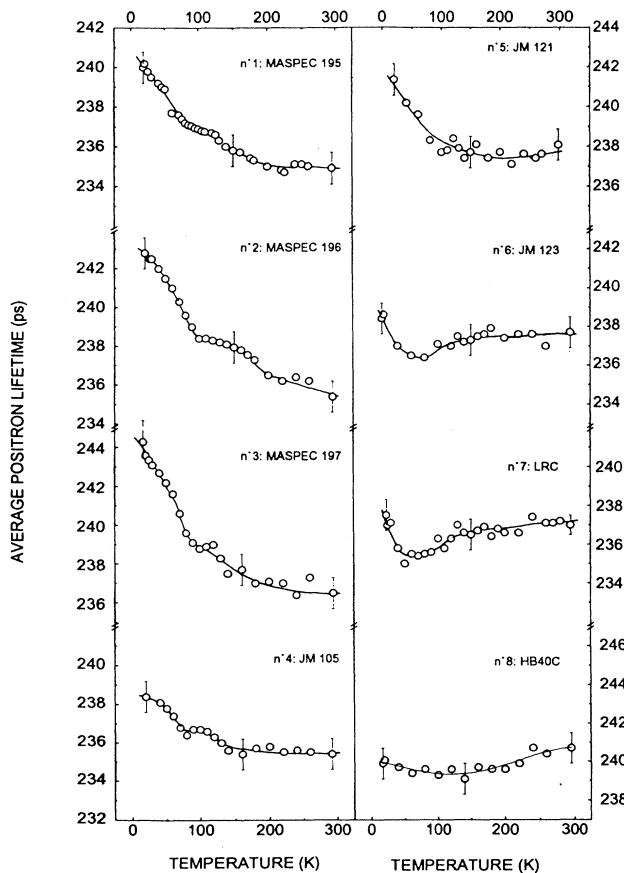


FIG. 4. Average positron lifetime measured in darkness as a function of temperature in eight SI GaAs crystals. Solid lines are guides for the eyes.

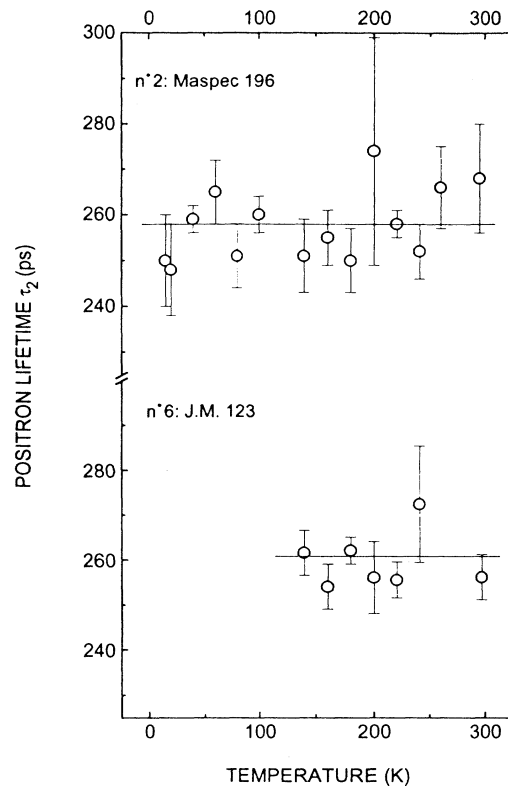


FIG. 5. Typical behavior of the long component τ_2 as a function of temperature in two different types of crystals.

sition is impossible from 20 K to about 100–150 K, whereafter it is easier. The lifetime τ_2 is then constant with a value 258 ± 5 ps.

B. Positron trapping at negative vacancies

The average positron lifetimes $\bar{\tau} = f(T)$ are all above the values $\tau_b = f(T)$ determined in *p*-type crystals and characteristic of annihilation in the lattice. This indicates that positrons are trapped at vacancy-type defects. We thus attribute the lifetime of 258 ps to vacancy-type defects. A lifetime of $\tau_d = 250$ –260 ps is typical for trapping at the open volume of a monovacancy.⁸ It can be shown² that the one-defect trapping model is valid when the expression $1/\tau_s = I_1/\tau_1 + I_2/\tau_2$ calculated from the decomposition of the spectra satisfies the equality $1/\tau_s = 1/\tau_b$. This is the case from 20 to 300 K for crystals Nos. 1–4, and only for temperatures close to 300 K for crystals Nos. 5–8. The positron-trapping rate at the detected monovacancy, K_d , can be calculated at all temperatures where the one-defect trapping model is verified by using the relation

$$K_d = \frac{1}{\tau_b} \frac{(\bar{\tau} - \tau_b)}{(\tau_d - \bar{\tau})}. \quad (3)$$

This is the case in crystals Nos. 1–4 from 20 to 300 K. Thus we use Eq. (3) to calculate K_d at all temperatures.

Its temperature dependence is shown in Fig. 6. K_d increases at low temperatures in a similar way in these four crystals: K_d varies like $T^{-0.5}$ from 20 to 130 K, and like $T^{-1.2}$ from 130 to 300 K. According to both theoretical and experimental basis,^{5,9} this indicates that the observed vacancies are negatively charged.

In an attempt to explain the large cross sections and the strong temperature dependence of positron trapping at negative vacancies, Puska, Corbel, and Nieminen⁵ have presented a model for positron trapping at isolated negative monovacancies. It is schematically shown in Fig. 7. In this model, the positron trapping can occur through two mechanisms. The first mechanism is a direct trapping from the delocalized state to the ground state at the vacancy, which occurs at a rate K_V . The second mechanism is an indirect, two-stage trapping. In the first stage, the delocalized positron is trapped at a Rydberg-like precursor state introduced by the Coulombic potential of the negative vacancy, with a rate K_R . The transition from this state to the ground state occurs at a rate η_R . Positrons can escape from the weakly bound precursor state and return to the delocalized state. When the localized and delocalized states are in thermal equilibrium, the detrapping rate δ_R is given by¹⁰

$$\frac{\delta_R}{K_R} = \frac{1}{C_v} \left[\frac{m + k_B T}{2\pi\hbar^2} \right]^{3/2} \exp \left[-\frac{E_R}{k_B T} \right], \quad (4)$$

where C_v is the vacancy concentration, $Nc = [m + k_B T / 2\pi\hbar^2]^{3/2}$ is the density of positron states per volume unit in the positron delocalized states band, and E_R is the binding energy of the precursor state. The global trapping rate observed experimentally can be expressed as the sum of the two mechanisms detailed above,

$$K_d = K_V(20 \text{ K}) \left[\frac{T}{20 \text{ K}} \right]^{-1/2} + \frac{K_R(20 \text{ K}) \left[\frac{T}{20 \text{ K}} \right]^{-1/2}}{1 + \frac{\mu_R(20 \text{ K})}{N\eta_R} \left[\frac{T}{20 \text{ K}} \right]^{-1/2} \left[\frac{m + k_B T}{2\pi\hbar^2} \right]^{3/2} \exp \left[-\frac{E_R}{k_B T} \right]}. \quad (6)$$

K_d then depends on four independent parameters: E_R , $\mu_R(20 \text{ K})/\eta_R$, $K_R(20 \text{ K})$, and $K_V(20 \text{ K})$.

Solid lines in Fig. 8 are least-square fits of Eq. (6) to the experimental trapping rates obtained by adjusting the four parameters. The fitted functions reproduce well the trends of the data. We found the same values in different crystals for the parameters independently of the vacancy concentration: $E_R = 70 \pm 30 \text{ meV}$, $\mu_R(20 \text{ K})/\eta_R = 10^4 - 10^5$, and $K_R(20 \text{ K})/K_V(20 \text{ K}) = \mu_R(20 \text{ K})/\mu_V(20 \text{ K}) \geq 5$. It is important to point out that these parameters are extremely sensitive to the shape of the experimental lifetime curves. We note that $\mu_R(20 \text{ K})$ and $\mu_V(20 \text{ K})$ verify

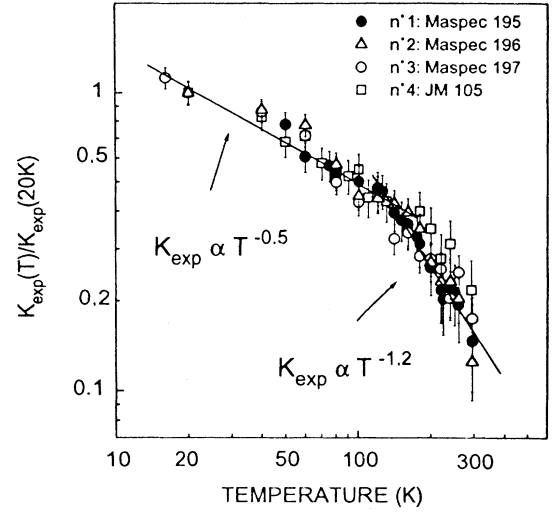


FIG. 6. Positron-trapping rate at gallium vacancies as a function of temperature in the four crystals where no negative ions are seen. The trapping rates are normalized to the value measured at 20 K.

the direct trapping and the indirect one:

$$K_d = K_V + \frac{K_R}{1 + \frac{\mu_R}{N\eta_R} \left[\frac{m + k_B T}{2\pi\hbar^2} \right]^{3/2} \exp \left[-\frac{E_R}{k_B T} \right]}, \quad (5)$$

where N is the number of atoms per volume unit in the perfect GaAs crystal, and μ_R is the trapping coefficient of the positron to the precursor state, related to K_R through $K_R = \mu_R C_v / N$. Assuming that K_R and K_V vary like $T^{-1/2}$, K_d can be expressed by

$\mu_R(20 \text{ K}) > \mu_V(20 \text{ K})$, which reflects that the overlapping of the delocalized positron wave function is larger with the Rydberg-like precursor state of the vacancy than with its ground state. The stronger decrease of K_d observed experimentally above 130 K in the four crystals is due to the thermal detrapping from the Rydberg-like precursor state. Our results show therefore that the experimental positron-trapping rate at a negative monovacancy in SI GaAs is well described by a model taking into account a two-stage capture mechanism, via a Rydberg-like precursor state introduced by the Coulombic potential of the vacancy. This had been also observed by Mäkinen *et al.*

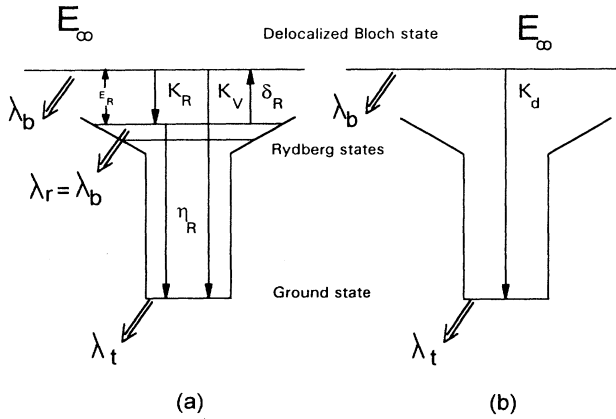


FIG. 7. A schematic picture of the two-stage positron capture mechanism (a), compared to the global trapping rate experimentally observed (b). E_R is the positron binding energy to the Rydberg state of the vacancy. The arrows represent the different transition rates. The symbols λ represent the positron annihilation rate from the different states.

for the negatively charged phosphorus-vacancy pair in silicon.¹¹

C. Identification of the vacancies

The Fermi level standing at midgap in semi-insulating materials, gallium vacancies are negative (V_{Ga}^{3-} or V_{Ga}^{2-} , depending on the authors) and arsenic vacancies are positive, (V_{As}^+).¹²⁻¹⁴ Thus we propose that the negative monovacancies we observe are related to gallium vacancies. We suggest that we observe the same vacancy SI GaAs crystals Nos. 1-4, characterized by a lifetime of

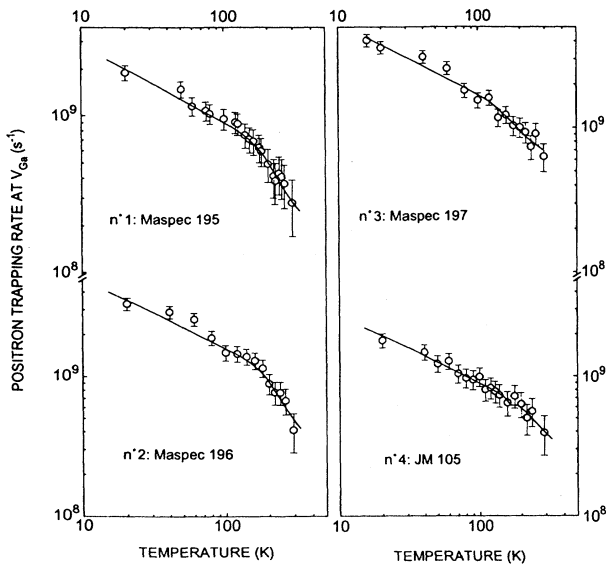


FIG. 8. Comparison between the experimental trapping rates at V_{Ga} (full circles) and the trapping rate calculated with Eq. (6) (solid lines), from the two-stage trapping mechanism (Ref. 5).

258 ps and a temperature dependence of the trapping coefficient calculated from Eq. (6). We associate it with the isolated gallium vacancy.

D. Evidence of negative ions

For the second group of crystals, Nos. 5-8, it is impossible to decompose the lifetime spectra in two components at low temperature. When the temperature is high enough to make it possible, the one-defect trapping model is not consistent below temperatures close to 300 K. This indicates that another defect traps positrons at low temperatures. This additional defect presents the following features: it becomes inefficient when the temperature increases, and its positron lifetime is very close to the bulk lifetime. The latter indicates that this trap has no open volume. We conclude that these traps are negative ions, and that at low temperature we observe a competition for positron trapping at negative ions and vacancies in these four crystals. These negative ions are shallow traps compared to vacancies. Above 100-150 K, the thermal detrapping from these shallow traps becomes significant, and they are no longer observed at 300 K. This was studied earlier in *n*-type GaAs (Ref. 15) and in electron-irradiated SI GaAs.⁸

To check that the temperature dependence of the lifetime in crystals Nos. 5-8 can be explained by the presence of negative ions, we compared the experimental data to an average lifetime calculated using a two-defect trapping model involving vacancies and negative ions. According to the two-defect trapping model, the average positron lifetime can be written as

$$\bar{\tau}_{\text{calc}} = \tau_d \frac{(\lambda_d + K_d) \left(\frac{\lambda_{\text{st}}}{K_{\text{st}}} + \frac{\delta_{\text{st}}}{K_{\text{st}}} \right) + \lambda_d}{(\lambda_b + K_d) \left(\frac{\lambda_{\text{st}}}{K_{\text{st}}} + \frac{\delta_{\text{st}}}{K_{\text{st}}} \right) + \lambda_{\text{st}}}, \quad (7)$$

where $\lambda_b = 1/\tau_b$ is the annihilation rate in the bulk, $\lambda_d = 1/\tau_d$ is the annihilation rate at the vacancy defect, K_d is the trapping rate at this vacancy, and $\lambda_{\text{st}} = 1/\tau_{\text{st}} = 1/\tau_b$ is the annihilation rate at the negative ions. The ratio $\delta_{\text{st}}/K_{\text{st}}$ of the detrapping rate to the trapping rate at the shallow traps has the same expression as the ratio δ_R/K_R , given for the Rydberg-like precursor state of trapping at the vacancy [see Eq. (4)]:

$$\frac{\delta_{\text{st}}}{K_{\text{st}}} = \frac{1}{C_{\text{st}}} \left[\frac{m + k_B T}{2\pi\hbar^2} \right]^{3/2} \exp \left[-\frac{E_b}{k_B T} \right], \quad (8)$$

where C_{st} is the concentration of the negative ions and E_b is the binding energy of the positrons to the negative ions. The lifetime data can be fitted by adjusting the values C_{st} , E_b , K_d (300 K), and K_{st} (20 K), and postulating the temperature dependences of the trapping rates K_d and K_{st} . For K_d , we take the same temperature dependence as that observed in crystals Nos. 1-4. We assume that K_{st} varies like $T^{-0.5}$, as predicted by the theory.⁵ The number of parameters to adjust can be reduced to two, C_{st} and E_b , because we have good estimations of the

values $K_d(300\text{ K})$ and $K_{st}(20\text{ K})$. The one-defect trapping model being verified at 300 K, the effect of the negative ions is weak at this temperature. $K_d(300\text{ K})$ is thus calculated in the first approximation using Eq. (3). At 20 K, the thermal detrapping from the negative ions, δ_{st} , can be neglected in the first approximation. $K_{st}(20\text{ K})$ is then calculated using a simple two-defect trapping model:

$$K_{st}(20\text{ K}) = \lambda_b \frac{\bar{\tau}(20\text{ K}) - \tau_b}{\tau_{st} - \bar{\tau}(20\text{ K})} - \frac{\bar{\tau}(20\text{ K}) - \tau_d}{\bar{\tau}(20\text{ K}) - \tau_{st}} K_d(20\text{ K}). \quad (9)$$

With these assumptions and the precision of the lifetime data, it is possible to fit the data for crystals Nos. 5 and 8 (see Fig. 9). This is not the case for crystals Nos. 6 and 7. In order to reproduce well the well-marked minimum observed for $\bar{\tau}$ around 50–100 K in these crystals, there is a need to use a temperature dependence for K_d which deviates from $T^{-0.5}$ as early as 30 K, with the form $T^{-0.9}$. This suggests that crystals Nos. 6 and 7 may contain vacancy-type defects which are different from those observed in crystals Nos. 1–5 and 8. Table II shows the parameters of the fits E_b and C_{st} for the four crystals Nos. 5–8. The binding energy E_b is in the range 50–100 meV, and the ion concentrations C_{st} vary from 10^{16} to $5 \times 10^{16}\text{ cm}^{-3}$. The values obtained for E_b are in good agreement

with the ionization energies of the Rydberg states⁶ calculated from the effective-mass theory,¹⁶ with a positron effective mass taken equal to m_0 . The negative ion concentrations are in reasonable agreement with the generally found acceptor concentrations in undoped bulk GaAs.¹

From Table II, where K_{st} , the trapping rate at negative ions, is given at 20 K, we can determine the positron-trapping coefficient at the negative ions, $\mu_{st} = K_{st}/C_{st}$, at 20 K. It has the same order of magnitude in the different crystals and its value $\mu_{st}(20\text{ K}) = (3 \pm 1) \times 10^{16}\text{ atm s}^{-1}$, is in the range of those predicted by the theory.⁵ This value is close to $\mu_{st}(20\text{ K}) = (1.1 \pm 0.3) \times 10^{16}\text{ atm s}^{-1}$ determined in electron-irradiated GaAs.¹⁷ As a mean value, we thus obtain $\mu_{st}(20\text{ K}) = (2 \pm 1) \times 10^{16}\text{ atm s}^{-1}$.

Various residual impurities and some intrinsic defects are believed to be negatively charged when the Fermi level stand at midgap.^{12–14} The negative ions observed could be impurities like C_{As}^- , Zn_{Ga}^- , Mo_{Ga}^- , or Fe_{Ga}^- . Among intrinsic defects, the gallium antisite Ga_{As}^{2-} is a good candidate.

E. Trapping coefficient and concentration of the Ga vacancy

The global positron-trapping coefficient $\mu_d = K_d/C_V$ at the Ga vacancy is determined at all temperatures from the parameters E_R , $\mu_R(20\text{ K})$, $\mu_V(20\text{ K})$, and η_R by

$$\mu_d = \mu_V(20\text{ K}) \left[\frac{T}{20\text{ K}} \right]^{-1/2} + \frac{\mu_R(20\text{ K}) \left[\frac{T}{20\text{ K}} \right]^{-1/2}}{1 + \frac{\mu_R(20\text{ K})}{N\eta_R} \left[\frac{T}{20\text{ K}} \right]^{-1/2} \left[\frac{m + k_B T}{2\pi\hbar^2} \right]^{3/2} \exp \left[-\frac{E_R}{k_B T} \right]}. \quad (10)$$

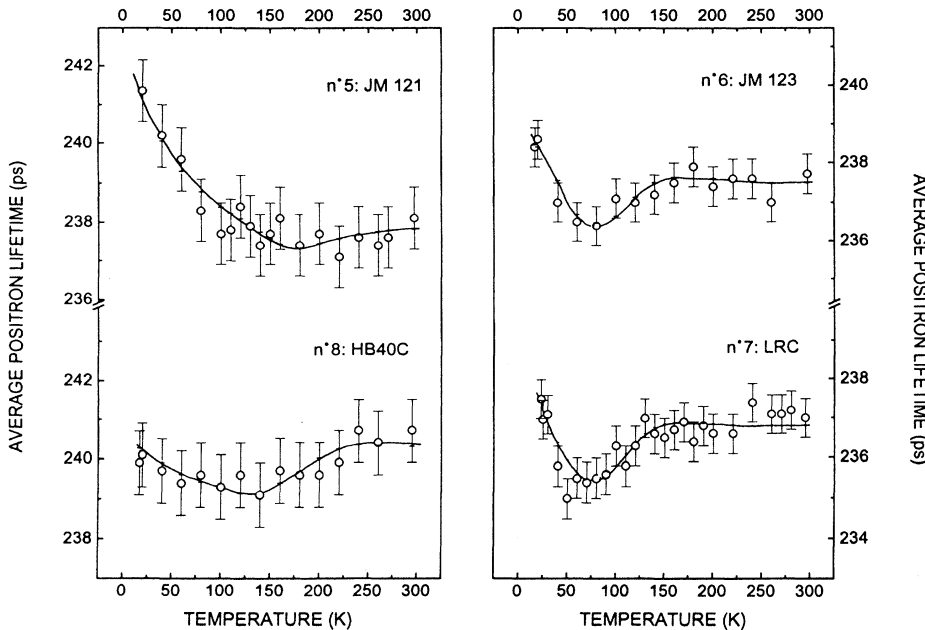


FIG. 9. Comparison between the experimental average lifetime (solid circles) and the average lifetime calculated with Eq. (8) (solid lines), from a trapping model including vacancies and negative ions. For crystals Nos. 6 and 7, the temperature dependence of the trapping rate at the vacancy is different than that observed in crystals Nos. 1–4 and used for calculating the average lifetime in crystals Nos. 5 and 8. The parameters of the adjustment are given in Table II.

TABLE II. Binding energy E_b and concentration C_{st} of the negative ions obtained by fitting the experimental lifetime data with a two-defect trapping model involving vacancies and negative ions. The positron-trapping rate K_{st} at the negative ions is estimated at 20 K, and the positron-trapping coefficient is calculated from C_{st} and K_{st} .

Crystal	E_b (meV)	C_{st} (10^{16} cm $^{-3}$)	K_{st} (20 K) (10^{10} s $^{-1}$)	μ_{st} (20 K) (10^{16} at s $^{-1}$)
SI-GaAs No. 5	100±20	1.4±0.5	0.57	1.8±0.5
SI-GaAs No. 8	90±20	4.3±0.8	2.28	2.4±0.5
SI-GaAs No. 6	50±15	3.9±0.8	2.64	3.1±0.6
SI-GaAs No. 7	60±15	3.6±0.8	2.62	3.2±0.8

Assuming that the positron-trapping coefficient at the Rydberg-like precursor state at the gallium vacancy is close to that at negative ions, $\mu_R(20\text{ K}) = (2 \pm 1) \times 10^{16}$ T s $^{-1}$, it is possible to determine μ_d in the crystals Nos. 1–4. First, from the fitted values of the ratios $\mu_R(20\text{ K})/\mu_V(20\text{ K})$ and $\mu_R(20\text{ K})/\eta_R$, we obtain η_R , the positron transition rate from the precursor state to the ground state in the vacancy. Its value is in the range 10^{10} – 10^{11} s $^{-1}$ as estimated by the theory.⁵ We obtain the values $\mu_d = (2.1 \pm 0.7) \times 10^{16}$ atm s $^{-1}$ at 20 K and $\mu_d = (3 \pm 1) \times 10^{15}$ atm s $^{-1}$ at 300 K. This latter value is of the same order as the value 1.3×10^{15} atm s $^{-1}$, determined for Ga vacancies in electron-irradiated SI GaAs from an estimation of the vacancy introduction rate.⁸ These values lead to V_{Ga} concentrations varying from 4×10^{15} to 8×10^{15} cm $^{-3}$ in crystals Nos. 1–4. Using the positron-trapping coefficient μ_d determined with these crystals, it is possible to calculate the vacancy concentration in the other four crystals at 300 K where the one-defect trapping model is verified. The detected concentrations vary from 10^{16} to 3×10^{16} cm $^{-3}$. The concentrations of both acceptors, gallium vacancies and negative ions, are higher than the concentrations of EL2 $^+$ measured in these samples and reported in Table I. Illumination experiments on this set of crystals reported else-

where¹⁸ have shown that under illumination positrons detect As vacancies in the range of concentration 10^{15} – 10^{16} cm $^{-3}$, indicating that donors other than EL2 should be taken into account in the compensation mechanism. The existence of other donors than EL2 had already been mentioned by Meyer *et al.*¹⁹

V. CONCLUSIONS

In this work, we have studied the positron lifetime in *p*-type and semi-insulating gallium arsenide in the temperature range 20–300 K. In *p*-type materials, with carrier concentrations varying from 5.4×10^{16} to 10^{19} cm $^{-3}$, no evidence of positron trapping at vacancies is observed. The temperature dependence of which the lattice expansion is associated to the positron-phonon coupling can explain the temperature dependence of the positron lifetime. Therefore, we ascribe the observed lifetime to delocalized positrons.

In SI GaAs, positrons detect negative vacancies and negative ions. Due to the Fermi-level position at midgap, we relate vacancy-type defects to gallium vacancies. The negative ions can be extrinsic acceptor impurities, as well as intrinsic acceptors as gallium antisites. The detected concentrations of these acceptors are in the range 10^{15} – 10^{16} cm $^{-3}$.

In six of the eight crystals which were studied, we observe a second lifetime $\tau_2 = 258 \pm 5$ ps that we ascribe to positron trapping at the isolated gallium vacancy, negatively charged. Positron trapping at this vacancy is characterized by a strong decrease of the positron-trapping coefficient as a function of temperature, with a change in the slope at about 130 K. This observation supports the two-stage positron capture model, where the attractive Coulomb potential between a positron and the negatively charged vacancy gives rise to Rydberg states acting as precursor states in the positron capture. We use the value of the positron-trapping coefficient measured for the negative ions to determine the global positron trapping coefficient at the gallium vacancy: $\mu(20\text{ K}) = (2.1 \pm 7) \times 10^{16}$ atm s $^{-1}$ and $\mu(300\text{ K}) = (3 \pm 1) \times 10^{15}$ atm s $^{-1}$.

- ¹G. M. Martin and S. Makram-Ebeid, in *Deep Centers in Semiconductors*, edited by S. T. Pantelides (Gordon and Breach, New York, 1986), Chap. 6.
- ²*Positrons in Solids*, edited by P. Hautojärvi, Topics in Current Physics Vol. 12 (Springer-Verlag, Heidelberg, 1979); *Positron Solid State Physics*, edited by W. Brandt and A. Dupasquier (North-Holland, Amsterdam, 1983).
- ³K. Saarinen, P. Hautojärvi, P. Lanki, and C. Corbel, Phys. Rev. B **44**, 10 585 (1991).
- ⁴M. J. Puska, C. Corbel, and R. M. Nieminen, Phys. Rev. B **38**, 9874 (1988).
- ⁵M. J. Puska, C. Corbel, and R. M. Nieminen, Phys. Rev. B **41**, 9980 (1990).
- ⁶C. Weyrizli, in *Zahlenwerte und Funktionen aus Naturwissenschaften und Technik*, edited by K.-H. Hellwege and O. Madelung, Landolt-Börnstein, New Series, Vol. 22 (Springer,

Heidelberg, 1989).

- ⁷M. J. Stott and R. N. West, J. Phys. F **8**, 635 (1978).
- ⁸C. Corbel, F. Pierre, K. Saarinen, P. Hautojärvi, and P. Moser, Phys. Rev. B **45**, 3386 (1992).
- ⁹J. Mäkinen, C. Corbel, P. Hautojärvi, P. Moser, and F. Pierre, Phys. Rev. B **39**, 10 162 (1989).
- ¹⁰M. Manninen and R. M. Nieminen, Appl. Phys. A **26**, 93 (1981).
- ¹¹J. Mäkinen, P. Hautojärvi, and C. Corbel, J. Phys. Condens. Matter **4**, 5137 (1992).
- ¹²G. A. Baraff and M. Schlüter, Phys. Rev. Lett. **55**, 1327 (1985).
- ¹³M. Puska, J. Phys. Condens. Matter **1**, 7347 (1989).
- ¹⁴H. Xu and W. Lindefelt, Phys. Rev. B **41**, 5975 (1990).
- ¹⁵K. Saarinen, P. Hautojärvi, A. Vehanen, R. Krause, and G. Dublek, Phys. Rev. B **39**, 5287 (1989).

¹⁶G. Burns, *Solid State Physics* (Academic, London, 1985).

¹⁷K. Saarinen, S. Kuisma, J. Mäkinen, P. Hautojärvi, M. Törnqvist, and C. Corbel, *Phys. Rev. B* **51**, 14 152 (1995).

¹⁸C. Le Berre, C. Corbel, R. Mih, M. R. Brozel, S. Tüzemen, S. Kuisma, K. Saarinen, P. Kautojärvi, and R. Fornari (unpub-

lished).

¹⁹B. K. Meyer, K. Krambrock, D. M. Hoffmann, and J.-M. Spaeth, in *Defect Control in Semiconductors*, edited by K. Sumino (Elsevier, Amsterdam, 1990).